9338–9352 *Nucleic Acids Research, 2018, Vol. 46, No. 18* *Published online 12 July 2018*
doi: 10.1093/nar/gky624

MouR controls the expression of the *Listeria monocytogenes* Agr system and mediates virulence

Jorge Pinheiro[1,2], Johnny Lisboa[3], Rita Pombinho[1,2], Filipe Carvalho[1,2], Alexis Carreaux[1,4], Cláudia Brito[1,2], Anna Pöntinen[5], Hannu Korkeala[5], Nuno M. S. dos Santos[3], João H. Morais-Cabral[6], Sandra Sousa[1,*] and Didier Cabanes[1,*]

[1]Group of Molecular Microbiology, IBMC – Institute for Molecular and Cell Biology; i3S – Institute for Research and Innovation in Health, Porto 4200-135, Portugal, [2]ICBAS- Instituto de Ciências Biomédicas Abel Salazar, University of Porto, Porto 4200-135, Portugal, [3]Group of Fish Immunology & Vaccinology, IBMC – Institute for Molecular and Cell Biology; i3S – Institute for Research and Innovation in Health, Porto 4200-135, Portugal, [4]SDV - UFR Sciences Du Vivant: Université Paris Diderot-Paris 7, Paris 75013, France, [5]Department of Food Hygiene and Environmental Health, Faculty of Veterinary Medicine, University of Helsinki, Helsinki 00014, Finland and [6]Group of Structural Biochemistry, IBMC – Institute for Molecular and Cell Biology; i3S – Institute for Research and Innovation in Health, Porto 4200-135, Portugal

Received February 12, 2018; Revised June 25, 2018; Editorial Decision June 26, 2018; Accepted June 28, 2018

ABSTRACT

The foodborne pathogen *Listeria monocytogenes* (*Lm*) causes invasive infection in susceptible animals and humans. To survive and proliferate within hosts, this facultative intracellular pathogen tightly coordinates the expression of a complex regulatory network that controls the expression of virulence factors. Here, we identified and characterized MouR, a novel virulence regulator of *Lm*. Through RNA-seq transcriptomic analysis, we determined the MouR regulon and demonstrated how MouR positively controls the expression of the Agr quorum sensing system (*agrBDCA*) of *Lm*. The MouR three-dimensional structure revealed a dimeric DNA-binding transcription factor belonging to the VanR class of the GntR superfamily of regulatory proteins. We also showed that by directly binding to the *agr* promoter region, MouR ultimately modulates chitinase activity and biofilm formation. Importantly, we demonstrated by *in vitro* cell invasion assays and *in vivo* mice infections the role of MouR in *Lm* virulence.

INTRODUCTION

Pathogenic bacteria depend on an arsenal of genes encoding virulence factors to successfully infect their host. During infection, by exerting specific functions, each virulence factor plays crucial roles ranging from cell invasion to nutrient acquisition and subversion of the immune system (1). While the expression of such factors is fundamental at a given time, their constitutive or over-expression is energetically wasteful and even harmful to the pathogen (2,3).

Thus, the tight regulation of virulence factors expression becomes a crucial mechanism for pathogen survival and fitness. Transcriptional regulators of virulence respond to various signals, both environmental and host-derived, and accordingly trigger a switch in the virulence factor expression pattern (4,5).

Listeria monocytogenes (*Lm*) is a Gram-positive bacterium and the causative agent of the systemic disease listeriosis. Although ubiquitous and commonly found growing in diverse environments, *Lm* switches from a saprophyte into a deadly pathogen (6,7), currently holding the highest mortality rate among foodborne pathogens in Europe (8). *Lm* is well equipped to survive the hostile conditions of the human digestive tract, invade both phagocytic and non-phagocytic cells, cross major biological barriers (intestinal, blood-brain and placental barriers), cause septicemia in immunocompromised individuals, infants and the elderly and, in the case of pregnant women, severely infect the foetus (9–11).

Virulence regulation of *Lm* greatly depends on the transcription regulator PrfA, which controls the expression of a broad list of genes, including major virulence factors and is thus regarded as the *Lm* master virulence regulator (12). Despite this, several other important regulators such as SigB (13), VirR (14), Hfq (15), MogR (16), DegU and GmaR (17,18) contribute, to a lesser extent, to the *Lm* virulence regulatory network.

The GntR family of proteins is a large group of transcription factors associated with the regulation of various

*To whom correspondence should be addressed. Tel: +351 226074923; Email: didier@ibmc.up.pt
Correspondence may also be addressed to Sandra Sousa. Tel: +351 226074924; Email: srsousa@ibmc.up.pt

biological processes in many diverse bacteria (19,20). Members of this group share a basic structure including a highly conserved DNA-binding domain at the N terminus, showing a characteristic helix-turn-helix (HTH) motif, and an effector binding/oligomerization (E-O) domain at the C terminus (21). Due to its higher diversity, the C terminus is used to categorize the diverse GntR sub-families (FadR, HutC, MocR, YtrA, AraR and PlmA) (19). FadR from *Escherichia coli* is one of the best characterized GntR regulators. FadR dimers bind to specific DNA sequences through the HTH motif, while acyl-CoA binding to the E-O domain causes dramatic conformational changes impairing DNA binding (22). FadR regulates fatty acid biosynthesis and degradation through activation and repression of several genes (23).

The accessory gene regulator (*agr*) locus encodes a bacterial communication system consisting of a quorum sensing module paired with a classical two-component system (24). First described in *Staphylococcus aureus,* the Agr system is found in many other Gram-positive bacteria (25). In *Lm*, it has been associated with survival and competitive advantage in soil, adhesion to surfaces and biofilm formation, invasion of mammalian cells, infectivity in the mouse model and global changes in gene expression (26–30). Interestingly, despite being the only quorum sensing system described in *Lm,* it appears that monitoring population density is not its main function (31) and the role of its quorum sensing properties is mostly unknown (32). Also, no regulator of the Agr system has been described so far for *Lm*, its autoregulation being the only regulatory mechanism proposed (26,28).

We previously provided the first comprehensive view of the genome expression of *Lm* directly in deep organs (spleen) of infected mice (7). This enabled us to identify and characterize novel virulence factors, otherwise difficult to predict (33–35). It also showed that the *in vivo* differential expression of the *Lm* genome is coordinated by a complex regulatory network, in particular through the upregulation of the two major virulence regulators, PrfA and VirR, and their downstream effectors (7). Interestingly, during mouse infection, *Lm* appears also to overexpress several new potential virulence regulators. Here, we identified a novel transcription factor—MouR—upregulated during infection and involved in the orchestration of *Lm* virulence regulation. Notably, we demonstrated that *mouR* encodes a transcriptional activator of the Agr system and is necessary for full virulence. We characterized MouR at the structural level, identified its regulon and demonstrated how it controls biofilm formation and *Lm* chitinase-dependent immune evasion, as well as revealed its role in *Lm* virulence.

MATERIALS AND METHODS

Bacterial strains and growth conditions

Strains used are detailed in Supplementary Table S1. *Lm* EGD-e (ATCC-BAA-679) (WT) and *E. coli* were routinely cultured in Brain Heart Infusion (BHI) and Lysogeny Broth (LB) (Difco), respectively, at 37°C aerobically with shaking. BHI-agar and LB-agar (Difco) plates were used for growth on solid media. To draw growth curves of *Lm* strains, overnight cultures were diluted 1:100 in fresh BHI and absorbance ($OD_{600\,nm}$) was measured every 30 min. When appropriate, antibiotics were added to the media: ampicillin 100 μg/ml, erythromycin 5 μg/ml and kanamycin 50 μg/ml.

Mutant construction and strain complementation

The deletion of *mouR* (*lmo0651*) from the *Lm* EGD-e WT strain was achieved by double homologous recombination using the suicide plasmid pMAD (36). The detailed procedure was previously described (34). The primers used are listed in Supplementary Table S2. Complementation of the Δ*mouR* mutant strain was performed by genomic reintroduction of the gene *in trans*, as described before (7). Complementation was mediated by the *Lm* specific integrative plasmid pIMK (37), through the construction of pIMK(*mouR*) (Supplementary Table S1).

Plasmid for protein overexpression

The coding region of *mouR* was C-terminally fused to a 6-His tag by in-frame restriction enzyme cloning into the pET28a expression vector, using the primers listed in Supplementary Table S2, to create pET28a(*mouR*-6His).

Site-directed mutagenesis

To create the MouR amino acid substitutions (R44A, R48A, Y80F, H133F and H134F), site-directed mutations were performed on pIMK(*mouR*) and/or pET28a(*mouR*-6His) using the QuikChange II XL Site-Directed Mutagenesis Kit (Agilent Technologies) according to the manufacturer's recommendations and with primers listed in Supplementary Table S2.

Bioinformatic analyses

Gene sequences were obtained from the Genbank database (38) and homologue searches were performed with the BLAST tool (39). Search of conserved protein domains and prediction of protein function were performed with the web-based PROSITE (40) and NCBI's Conserved Domain Database (41) tools. Comparative analyses of protein sequences was conducted in MEGA7: Molecular Evolutionary Genetics Analysis version 7.0 (42).

RNA isolation and RT-qPCR

Lm cultures were grown in BHI to exponential phase ($OD_{600\,nm}$ = 1.0) and total RNA isolated by the phenol-chloroform method described elsewhere (43), with modifications as described next. After lysis, RNA purification was performed using the TripleXtractor reagent (Grisp, Porto) following the manufacturer's recommendations. DNA was eliminated by DNase treatment (Turbo DNA-free, Ambion) and RNA purity and integrity was verified by 1% (w/v) agarose gel electrophoresis and Experion Automated Electrophoresis System (Bio-Rad Laboratories). One μg of RNA was reverse-transcribed into cDNA using a random hexamer cocktail-based kit (iScript Kit, Bio-Rad Laboratories). qPCR was performed on one μg of cDNA in a 20 μl

reaction volume using the iTaq™ Universal SYBR® Green Supermix (Bio-Rad Laboratories) and a real-time PCR detection system (iQ5, Bio-Rad Laboratories) with the following cycling protocol: 1 cycle at 95°C (3 min); 40 cycles at 95°C (10 s), 56°C (20 s) and 72°C (20 s). Primers are listed in Supplementary Table S2. Each group comprises three biological replicates each with three technical replicates. Data were normalized to that of a reference housekeeping gene (16S rRNA) and analyzed by the comparative threshold (ΔΔCt) method.

RNA-seq

DNA-free total RNAs were depleted for rRNA species by processing with MICROBExpress Bacterial mRNA Enrichment Kit (Ambion) following the manufacturer's instructions. Efficient enrichment was verified by Experion Automated Electrophoresis System (Bio-Rad Laboratories) virtual gel analysis and Qubit 3.0 Fluorometer (Thermo Fisher Scientific) analysis. Sequencing of mRNAs was performed using the Ion Total RNA-Seq Kit v2 (Thermo Fisher Scientific) and quality control for RNA fragmentation and library construction was assessed by Qubit 3.0 Fluorometer (Thermo Fisher Scientific) and 2200 TapeStation (Agilent) analyses. Template preparation was achieved with an Ion Chef system (Thermo Fisher Scientific) and sample sequencing was done in triplicates with an Ion Proton System (Thermo Fisher Scientific). Generation of sequence reads and read trimming and filtering was done with Torrent Suite v4.4 software with a FileExporter v4.4 plugin for generation of FASTQ/BAM files. To assess differentially expressed genes between *Lm* WT and Δ*mouR* mutant strain, sequencing reads were aligned to the reference genome sequence of *Listeria monocytogenes* EGD-e (RefSeq: GCF_000196035.1, GenBank: GCA_000196035.1, assembly ASM19603v1 -http://www.ncbi.nlm.nih.gov/assembly/GCF_000196035.1) using the aligner TopHat2 (44). After transcript assembly, the relative abundance of each transcript was estimated by calculation of the metric fragments per kilobase of transcript per million mapped reads (FPKM) (45) using Cufflinks and Cuffdiff tools (46). Statistical significance was attributed to transcripts with fold change of expression higher than 2 or lower than 0.5, a *P*-value below 0.5 and an FDR-adjusted *P*-value below 0.1. Sequencing results are available on the GEO database (https://www.ncbi.nlm.nih.gov/geo/) under the accession number GSE106833.

Protein purification

Purification of 6xHis-tagged MouR and MouR(R44/48A) (Supplementary Table S1) proteins was performed by *E. coli* heterologous overexpression and chromatography as described elsewhere (47) with some modifications. Briefly, the growth of *E. coli* BL21(DE3), harbouring either pET28a(*mouR*-6His) or pET28a(*mouR*(R44/48A)), for 3 h at 37°C with agitation in LB supplemented with 0.5 M IPTG was determined as a favorable condition for high protein expression. Cultures were inoculated at 1:50 with an over-night culture pelleted by centrifugation at 200 rpm and re-suspended in LB. One litre of culture was grown and lysed with a French Pressure Cell Press (Thermo) at 12 000 psi. Proteins were trapped in a nickel-based matrix (Ni-NTA Agarose, Qiagen) and eluted with imidazole in a low-pressure liquid chromatography system (BioLogic DuoFlow QuadTec10 System, Bio-Rad). Lastly, imidazole was removed by membrane dialysis (Spectra/Por Dialysis Membrane, SpectrumLabs) and protein was concentrated by Vivaspin (Sartorius Stedim Biotech) column centrifugation. For expression and purification of SeMet-MouR, *E. coli* B834(DE3) harboring pET28a(*mouR*-6His) was grown in 40 ml of LB overnight at 37°C, collected and washed three times with sterile deionized water and finally used to inoculate 1 l of SelenoMethionine Medium (Molecular Dimensions). Purification was performed following the procedure described for the native protein.

Crystallization and structure determination of MouR

Both native and SeMet-substituted MouR proteins were stored in 50 mM Tris–HCl pH 8.0, 300 mM NaCl. Native crystals were grown at 20°C from a 0.1:0.1 μl mixture of a 10 mg/ml protein solution with a crystallization solution composed of 1.5 M lithium sulfate, 100 mM sodium Hepes pH 7.5. SeMet-MouR crystals were grown from a mixture of 6 mg/ml protein solution with a crystallization solution composed of 3 M NaCl, 100 mM Tris pH 8.5. Crystals were flash-frozen directly in liquid nitrogen. Native and SeMet diffraction data were recorded on beamlines Proxima 2A (Soleil, Gif-sur-Yvette, France) and ID29 (ESRF, Grenoble, France). The structure was determined by the SAD (Single wavelength Anomalous Dispersion) method using the anomalous signal from the selenium element. Data were processed with XDS (48) in space group P41, with two copies per asymmetric unit. All expected Se sites (eight by monomer) were found with SHELXD using reflections in the 50–3.5 Å resolution range (49). Refinement of Se atom positions, phasing and density modification were performed with Phenix-EP. The high quality of the experimental phases allowed automatic building (Autobuild program) of most of the protein model. The model was refined against the 2.2 Å native data set using PHENIX (50). The final model contains residues 3–217 from both monomers. In addition, 85 water molecules, 10 sulfate ions, one 4-(2-hydroxyethyl)-1-piperazineethanesulfonic acid and six ethylene-glycol could be modelled into the electron density maps. Statistics for data collection and refinement are summarized in Supplementary Table S3. Data of the reported crystal structure was deposited in the Protein Data Bank (PDB) (https://www.rcsb.org) under the ID: 6EP3.

Electrophoretic mobility shift assays

Protein-DNA binding was set up in 20 μl reactions containing 240 ng of DNA synthesized with primers described in Supplementary Table S2, binding buffer (50 mM HEPES pH 7.5, 500 mM NaCl, 1mM EDTA, 0.1 mM DTT, 5% glycerol, 0.01 mg/ml BSA) and increasing amounts of purified protein as previously described (35). DNA was first incubated in binding buffer for 5 min followed by gentle mixing of the protein and 20 min incubation at room temperature. The total reaction was loaded into a 10% acrylamide

native gel and ran in TAE buffer. The gel was stained for 10 min in a 0.01% GreenSafe Premium (NZYTech) TAE buffer solution and imaged in a GelDoc XR+ System (Bio-Rad Laboratories).

Chitin hydrolysis assay

Evaluation of chitinase activity was performed as described (51). Five gram of shrimp shell chitin (Sigma-Aldrich) were pre-treated with 50 ml of HCl (37%) overnight. Treated chitin was adjusted to pH 8 with NaOH and pelleted at 8300 g for 5 min, washed with ultrapure water seven times and used to supplement LB-agar plates (6 mg/ml). 10 μl of *Lm* overnight cultures were spotted on the plates and incubated at 30°C for 6 days. Chitin hydrolysis was evaluated by measuring the radius of the degradation halo.

Biofilm formation

Lm ability to form biofilm was evaluated by crystal violet turbidimetry assay (52). Overnight cultures of *Lm* were diluted 1:100 in BHI and 100 μl (octaplicates) were transferred to sterile 96-well PVC plates (Corning) and incubated at 30°C for 20 h. Wells filled with sterile BHI served as control. Media was removed and loose bacteria were washed three times with distilled water. Air dried wells (30 min) were filled with 150 μl of 0.5% crystal violet (BDH) for 45 min. Excess stain was washed three times with distilled water, the plate was air dried and biofilm-associated crystal violet was re-suspended in 200 μl of 99% ethanol. 100 μl of each well was transferred to a new plate and the $OD_{595\,nm}$ was measured in a plate reader (μQuant, Biotek).

Biofilm formation was also assessed as described (53). *Lm* overnight cultures were diluted 1:100 in fresh BHI and were grown at 30°C on glass coverslips (22 × 22 cm) submerged in a six-well plate. Three days post-incubation, the coverslips were washed three times with distilled water, fixed with 4% glutaraldehyde during 2 h and stained with 0.1% acridine orange for 15 min. Coverslips were mounted onto microscope slides with Aqua-Poly/Mount (Polysciences) and examined under a confocal laser-scanning microscope (Leica SP5II). Sections were taken every 0.5 μm and processed using Fiji-ImageJ (54,55). Biofilm thickness was calculated using Leica SP5II software.

Cell invasion assays

Human cell lines invasion assays were performed as described (33). Briefly, cells were grown to confluency in Eagle's medium with L-glutamine (EMEM) (Lonza), supplemented with nonessential amino acids (Lonza), sodium pyruvate (Lonza) and 20% fetal bovine serum (FBS, Biowest) (Caco-2, ATCC HTB-37) or in Dulbecco's modified Eagle's medium (DMEM) with glucose (4.5 g/l) and L-glutamine (Lonza), supplemented with 10% FBS (HeLa, ATCC CCL-2 and Jeg-3, ATCC HTB-36). *Lm* was grown to exponential phase, washed and inoculated at a multiplicity of infection of 75 for 1 h. Cells were incubated with medium supplemented with 20 μg/ml gentamycin (Lonza) for 1h 30 min to eliminate extracellular bacteria, washed and lyzed with 0.2% Triton X100. Bacterial suspensions were serially diluted and plated on BHI-agar plates for CFU determination.

Intracellular multiplication

Assays of intracellular multiplication in mouse macrophages were performed as described (33). RAW 264.7 cells (ATCC TIB-71, ∼2×10^5/well) were propagated in DMEM (Lonza) supplemented with 10% FBS (Biowest), infected as described above with exponential phase bacteria at a multiplicity of infection of 10 for 30 min and treated afterwards with 20 μg/ml gentamicin. At, 2, 5, 7 and 20 h post-infection cells were washed with PBS, lysed in cold 0.2% Triton X-100 and bacterial suspensions were serially diluted and plated on BHI-agar plates for CFU determination.

Animal infections

Animal infections were performed with 6–9-week-old specific pathogen-free female BALB/c mice (Charles River Laboratories) maintained at the IBMC animal facilities, in high efficiency particulate air (HEPA) filter-bearing cages under 12 h light cycles and in an *ad libitum* regiment of sterile chow and autoclaved water. Intravenous infections were performed by inoculation of 10^4 CFUs through tail vein injection as described (56). For oral infections mice were starved for 8–12 h before the procedure and inoculated with 2×10^9 CFUs (in PBS with 150 mg/ml $CaCO_3$) by gavage. Mice were sacrificed by general anaesthesia 72 h post-infection and the liver, spleen and Peyer's patches of each animal were aseptically removed. Peyer's patches were washed twice with EMEM, incubated in EMEM supplemented with 100 μg/ml gentamycin (Lonza) for 1 h, and washed twice with EMEM and once with PBS. Organs were homogenized in PBS and homogenates were serial diluted and plated on BHI-agar plates for livers and spleens or on *Listeria* Selective Agar (Oxoid) plates supplemented with *Listeria* Selective Supplement (Oxoid) for Peyer's patches. Animal procedures were in agreement with the guidelines of the European Commission for the handling of laboratory animals (directive 2010/63/EU), the Portuguese legislation for the use of animals for scientific purposes (Decreto-Lei 113/2013), and were approved by the IBMC Animal Ethics Committee as well as by the Direcção Geral de Alimentação e Veterinária, the Portuguese authority for animal protection, under license 015302.

Statistical analyses

Statistical analyses were performed with the software Prism 7 (GraphPad Software). Unpaired two-tailed Student's *t*-test was used to compare the means of two groups; one-way ANOVA was used with Tukey's post-hoc test for pairwise comparison of means from more than two groups, or with Dunnett's post-hoc test for comparison of means relative to the mean of a control group. Differences with a calculated *P*-value above 0.05 were considered non-significant and statistically significant differences were noted as follows: $*P < 0.05$; $**P < 0.01$; $***P < 0.001$.

RESULTS

lmo0651 encodes a putative transcription regulator

In a previous study, we reported the transcriptome profiling of *Lm* while infecting the mouse spleen and identified the gene *lmo0651* as highly expressed during spleen infection when compared to growth in BHI medium (≅100-fold) (7). In addition, *lmo0651* was also previously shown to be upregulated when *Lm* was infecting the mouse intestinal lumen or incubated in human blood (57). Through bioinformatics and database analysis, the Lmo0651 protein was predicted as a transcriptional regulator containing a putative typical GntR winged HTH DNA-binding domain (19) (Figure 1A). Protein sequence alignments showed that Lmo0651 appears to be conserved across the *Listeria* genus, found in the genome of almost all pathogenic and non-pathogenic species and serogroups (Figure 1B and S3A). However, it has no close relatives outside the genus, the closest hit being a protein from *Isobaculum melis* annotated as a 'DNA-binding transcriptional regulator, GntR family' (Figure 1B). Although flanked by two predicted transcription terminators, *lmo0651* appears to be part of an operon (*lmo0648 to lmo0651*) (57) comprising genes encoding potential membrane proteins (*lmo0648 and lmo0650*) or similar to transcription regulators (*lmo0649 and lmo0651*) (Figure 1C).

MouR is the transcriptional activator of the Agr system

To study the role of Lmo0651 as a regulator and identify genes under its control, we designed an RNA-seq-based experiment to assess the genome-wide expression of both *Lm* EGD-e WT and the Δ*lmo0651* deletion mutant in exponential growth phase in BHI at 37°C. When compared to the WT strain, six transcripts (*agrD, agrB, agrC, agrA, fruA, lmo0278*) appeared less abundant in the Δ*lmo0651* mutant, while only one (*lhrA*) was more abundant (Figure 2A), suggesting that Lmo0651 acts mainly as a transcriptional activator. Four of these genes (*agrD, agrB, agrC* and *agrA*) are clustered in an operon located 639 kb away from *lmo0651* and encoding the components of the conserved Agr quorum sensing system of *Lm* (32,58) (Supplementary Figure S3B–E), which is involved in survival in the environment, biofilm formation and virulence (26–28,30). *lhrA* is a non-coding short RNA (ncRNA) negatively regulated by Agr (51) and known to regulate several genes, including the chitinase-coding gene *chiA* through mRNA binding and interference with ribosome recruitment (59,60). In addition to Agr system related genes, *fruA* and *lmo0278* were also less expressed in absence of Lmo0651 (Figure 2A). These genes are related to sugar uptake, *fruA* encodes one of the components of a fructose-specific phosphotransferase system and *lmo0278* encodes a maltose uptake ABC transporter (61,62). Both genes seem to be essentially related to metabolic pathways and, furthermore, they appear to have a complex dynamic type of regulation since they seem prone to be similarly regulated in comparative genome-wide transcriptomes (7,57,63,64).

We further confirmed our RNA-seq results by RT-qPCR. We selected a subset of up- and down-regulated genes and performed qPCR on cDNA from WT and Δ*lmo0651* bacteria grown to exponential phase. RT-qPCR results and RNA-seq data exhibited a very strong Pearson correlation coefficient ($R^2 = 0.93$) (Figure 2B), therefore validating the differential expression levels detected by transcriptomics.

Together, these results pointed Lmo0651, renamed MouR, as the transcriptional activator of the Agr system.

MouR is a dimeric GntR protein

To further explore the function of MouR, we purified MouR and resolved its three-dimensional structure (Figure 3). The crystal structure of MouR was determined by the SAD method using SeMet-substituted protein. The atomic model was refined against a native data set to 2.2 Å resolution (Supplementary Table S3). The final model of MouR shows a homodimer that includes residues Asn3 to Arg217 for both subunits and three histidines from the His-Tag for one of the subunits (Figure 3A). The subunits in the homodimer display a RMSD of 1.5 Å (http://zhanglab.ccmb.med.umich.edu/TM-align/) (65). The protein presents the fold of the GntR superfamily of dimeric transcription factors with each subunit composed by two domains (Figure 3B). The N-terminal domain of MouR (Asn3–Cys73) is a winged-helix dsDNA-binding domain, characteristic of the GntR family, and includes the canonical HTH DNA-binding motif (α1–α2–α3) followed by a β-hairpin (β1–β2). The FadR C-terminal putative regulatory domain (FCD domain), encompassing residues Val75–Arg217, contains an antiparallel array of six α-helices (α4–α5–α6–α7–α8–α9) that form a barrel-like structure. The presence of only six α-helices within the FCD domain classifies MouR as a member of the VanR subclass of the FadR family of GntR regulators. The dimer interface is mediated exclusively by helix α4 of the FCD domain (Figure 3A and C), burying a surface of ∼1150 $Å^2$ per monomer (calculated with 'Protein interfaces and assemblies' service PISA at the European Bioinformatics Institute; http://www.ebi.ac.uk/msd-srv/prot_int/pistart.html) (66). Residues that contribute to the dimerization are listed in Supplementary Table S4, together with an estimate of the accessibility of individual residues in the dimer versus the monomer. Interface residues are located mainly on α4 and the loop between α6 and α7 (Figure 3C). The interface involves apolar contacts mediated by Ile89, Phe90, Ala93 and Ile152, a network of hydrogen bonds and electrostatic interactions involving Gln82, Glu85, Thr86, Lys97, Glu145 and Gln149 (Figure 3C). It is known that the regulatory domains of the FadR family bind small organic ligands leading to conformational changes that reorient their winged-helix domains and affect DNA binding (67,68). Analysis of the electron density map revealed an internal polar cavity within the FCD domain, suggesting a putative ligand-binding site (Figure 3A and D). FCD domains commonly display three conserved histidines that interact and bind a metal ion in the cavity (68). The density map of MouR structure revealed that only two histidines (His133 and His134) are conserved whereas a tyrosine (Tyr80) is present in place of the third histidine (Figure 3D). In addition, this pocket is large, with a volume of ∼170 $Å^3$ and the electron-density map shows unexplained density in the cavity where a molecule of ethylene glycol, the cryoprotectant used to freeze the crystal, was modelled. Alto-

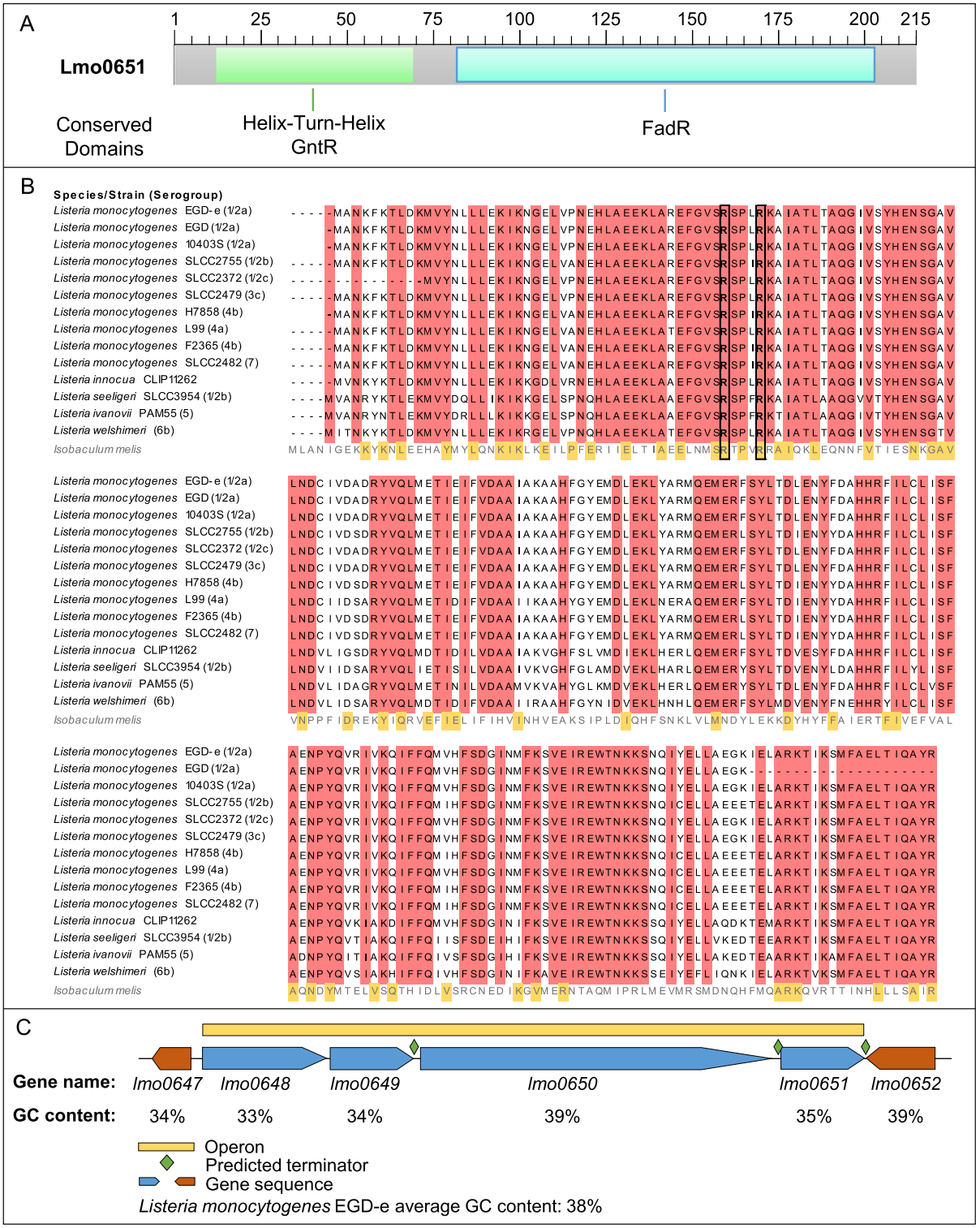

Figure 1. *lmo0651* encodes a novel GntR transcription factor. (**A**) Bioinformatic analysis predicts the locus *lmo0651* of *Lm* to encode a transcription factor with a typical N-terminal DNA-binding winged helix-turn-helix GntR domain and a C-terminal FadR domain. (**B**) Alignment of protein sequence of Lmo0651 with orthologs from other *Lm* strains and *Listeria* species, with conserved amino acid residues highlighted in red. Amino acids conserved between *Lm* EGD-e Lmo0651 and the putative GntR transcriptional regulator in *Isobaculum melis* (the closest relative outside of the *Listeria* genus found by BLAST analysis) are marked in yellow. Critical DNA-binding arginines are highlighted with black boxes. (**C**) Genomic organization of the *mouR* region in *Lm* EGD-e.

A

Gene	Fold change†
agrD‡	- 144,19
agrB	- 77,76
agrC	- 29,15
agrA	- 20,92
fruA	- 5,04
lmo0278	- 3,87
lhrA	+ 7,32

† Fold change values refer to expression of genes significantly regulated in *Lm* Δ*mouR* as shown by *in vitro* transcriptome vs. WT.

‡ Gene did not make statistical stringency cutoff.

B

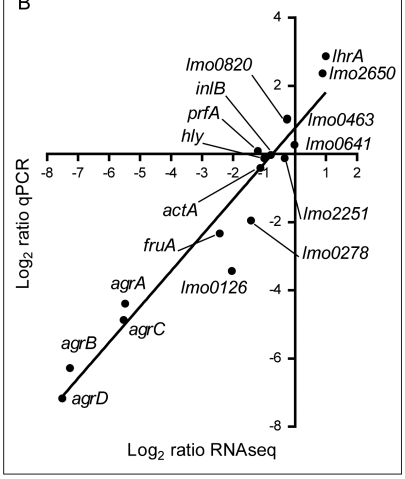

Figure 2. Genes differently regulated in Δ*mouR in vitro.* (**A**) Fold change of the expression of genes regulated by MouR as shown by RNA-seq. (**B**) Validation of RNA-seq transcriptomics data by RT-qPCR. Data represented as Log2 of fold change between *in vitro* gene expression of *Lm* WT and Δ*mouR* in exponential growth in BHI at 37°C as measured by RNA-seq and RT-qPCR.

gether this suggests that the pocket binds a small-molecule instead of a metal.

MouR-dsDNA complex model

The GntR superfamily of dimeric transcription factors is characterized by the presence of an N-terminal winged-helix DNA-binding domain. Three structures of FadR-dsDNA complex are available on PDB: two from *E.coli* (ID: 1HW2 and 1H9T) (22,69) and one from *Vibrio cholera* (ID: 4P9U) (70). These FadR proteins in complex with DNA present an identical structural arrangement of their winged-helix domains and conserved DNA-interacting amino acid residues. The superimposition of MouR winged-helix domain onto FadR-dsDNA complexes (ID: 1HW2, 1H9T and 4P9U) shows that it has a similar structure. Therefore, we modelled the MouR-dsDNA complex using the FadR-dsDNA complex from *E. coli* (ID: 1HW2) (Figure 4A). Analysis of the model strongly shows that Arg44 and Arg48 on the α3-helix appear ready to interact with DNA (Figure 4B). These two arginine residues are conserved in the GntR superfamily (Figure 1B), supporting their involvement in the binding to DNA. Among the other *E. coli* FadR (ID: IHW2) residues (Arg35, His65 and Lys67) involved in DNA contact, only the histidine (His63) is conserved in MouR, Arg35 being replaced by the Lys35. However, in our model these residues do not contact with DNA (Supplementary Figure S1), probably because the MouR protein will undergo structural adjustments when bound to DNA, accommodating the interaction of those amino acid residues with the DNA strand. On the other hand, this model shows that MouR Lys49 is also close to the major groove of the DNA and may also be involved in the interaction (Figure 4B). Although all known structures of winged-helix domain are very similar, their mode of interaction with dsDNA can vary greatly. While the majority of these interactions involve the α3–helix binding in the major groove of the DNA (71), our model of the MouR–dsDNA complex (Figure 4A) suggests that only the top of this helix is implicated in the interaction with dsDNA (Figure 4B).

MouR positively regulates the expression of the *agr* locus by binding to the operon promoter

Based on MouR structure analysis, we hypothesized that the α3-helix and in particular the conserved Arg44 and Arg48 residues would be essential for its ability to bind target DNA and, thus, crucial for its activity as a transcriptional regulator. To test this, we engineered an *Lm* strain to express, on a Δ*mouR* background, a mutated version of MouR in which Arg44 and Arg48 were replaced by alanine residues (*Lm* Δ*mouR*+*mouR*(R44/48A)). We confirmed that *mouR*(R44/48A) is expressed in this strain at levels comparable to *mouR* in the WT strain (Supplementary Figure S2), and analyzed the expression of MouR-regulated genes in the WT, Δ*mouR,* Δ*mouR*+*mouR* and Δ*mouR*+*mouR*(R44/48A) strains. We observed that in the Δ*mouR* strain the expression of the four *agr* genes was highly repressed while *lhrA* was upregulated (Figure 5A), as detected by RNA-seq. In the Δ*mouR*+*mouR* complemented strain the expression of all five genes was restored back to levels comparable to those of the WT (Figure 5A), definitively demonstrating the role of MouR in the expression of the *agr* locus and *lhrA*. Inversely, the Δ*mouR*+*mouR*(R44/48A) strain exhibited expression levels of *agr* genes similar to those observed for Δ*mouR* (Figure 5A). This strongly suggests that these conserved arginine residues at the N terminus of MouR are crucial for the transcriptional activation of the *agr* genes.

To investigate whether MouR controls the expression of the *agr* locus by direct binding of the operon promoter, we performed electrophoretic mobility shift assays to test protein-DNA interactions. We observed that increasing amounts of MouR were able to delay the migration of the band corresponding to the *agr* promoter (P*agr*), 0.2 μM of MouR being sufficient to delay the *agr* promoter mobility (Figure 5B). Furthermore, increasing amounts of the mutated MouR(R44/48A) variant failed to delay P*agr* migration, clearly indicating that the arginine residues are essential for the binding of MouR to the *agr* locus promoter. As controls, we used P*agr* with a purified unrelated regulator (Lmo0443), or mixed MouR with its own promoter region. In neither condition, we were able to detect a band

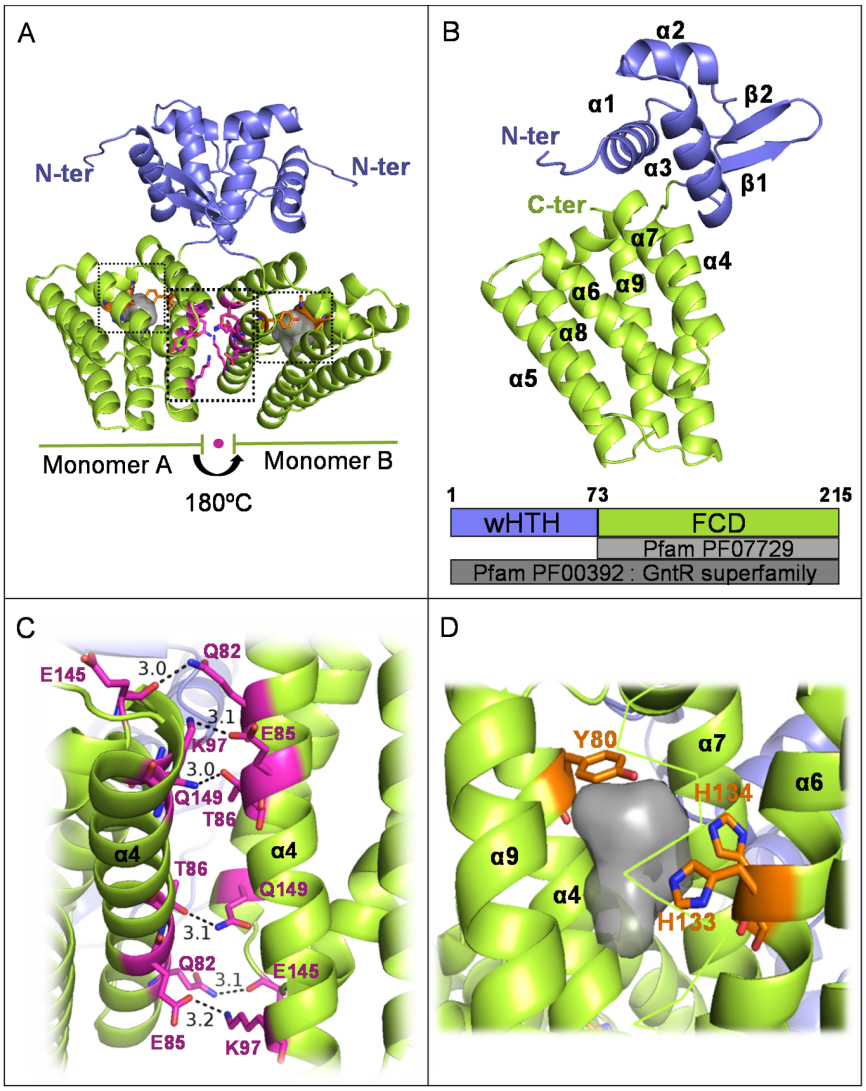

Figure 3. MouR structure and dimerization interface. (**A**) Ribbon representation of MouR structure. Dimerization interface and ligand binding cavities indicated by dashed-lined boxes. (**B**) Top: ribbon representation of the MouR subunit structure. The N and C termini and secondary structure elements are indicated. Colour code: blue, winged HTH domain; green, FCD domain. Bottom: linear representation of MouR structural domains according to Pfam (color code as the top). (**C**) The dimerization interface is enlarged to show some of the residues involved in the interaction (represented as magenta sticks). Hydrogen bonds are represented by dashed lines, and distances between residues are indicated in Å. (**D**) Highlight of the putative ligand-binding cavity of MouR (gray surface) with the conserved residues potentially relevant for ligand binding shown as orange sticks.

shift (Figure 5B), demonstrating that MouR acts as a DNA-binding transcription factor with specific affinity to the promoter of the *agr* operon.

Above, our analysis of the MouR structure revealed an internal polar cavity within the FCD domain, suggesting a putative ligand-binding site with two conserved histidines (His133 and His134) and a tyrosine (Tyr80) susceptible to interact with a potential ligand in the cavity (Figure 3D). To evaluate if the residues oriented towards the putative C-terminal ligand-binding cavity play a role in the MouR-dependent transcriptional activation of *agr* genes, we engineered *Lm* Δ*mouR* strains to express MouR with the residue substitutions: Y80F (*Lm* Δ*mouR*+*mouR*(Y80F)), H133F (*Lm* Δ*mouR*+*mouR*(H133F)) and H134F (*Lm* Δ*mouR*+*mouR*(H134F)). These substitutions alter the physical-chemical properties of the residues lining the cavity by decreasing the polar character of the cavity and reducing the availability of hydrogen-bond partners. We confirmed that *mouR* is expressed in these strains at levels comparable to the WT (Supplementary Figure S2). The expression of *agrB* was analyzed by RT-qPCR in these strains as compared to the WT. Our data showed that *agrB* expression in the mutant strains was not significantly different from the WT strain, indicating that none of the mutations impaired the ability of MouR to activate *agrB* expression (Figure 5C).

MouR regulates chitinase activity and biofilm formation

While the Agr system has not been deeply characterized in *Lm*, it was consistently associated with *Lm* chitinase activity and capacity to develop a biofilm (28,51). We thus an-

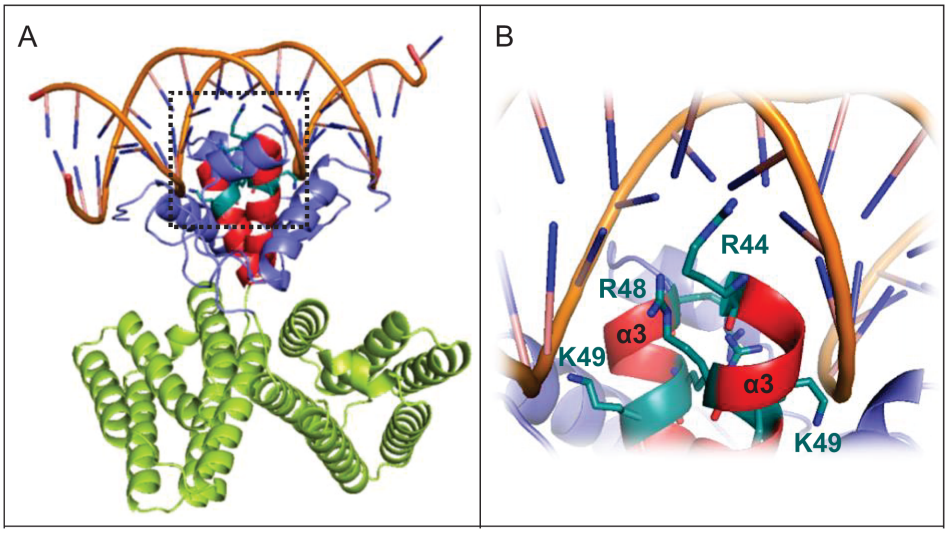

Figure 4. Model of MouR-dsDNA complex. (**A**) Ribbon representation of the modelled MouR–DNA complex. The DNA is modeled based on the superposition of the FadR–DNA complex (PDB ID: 1HW2) onto the winged-HTH domain of MouR. **(B)** The overall architecture of the winged-HTH domain of MouR (shown in blue), with putative DNA-binding residues shown (represented as sticks). The helix (α3) involved in the interaction with DNA is colored in red.

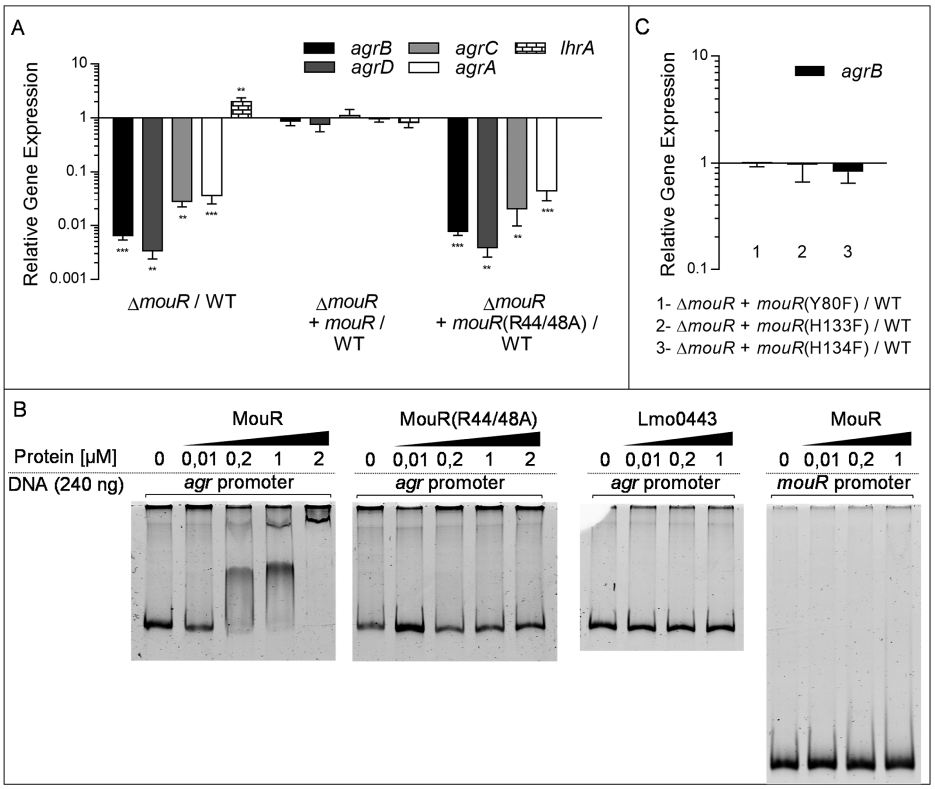

Figure 5. MouR positively regulates the expression of the *agr* locus by directly binding to the operon promoter. (**A**) Expression of *agr* genes and the ncRNA *lhrA* determined by RT-qPCR performed with total RNA isolated from *Lm* WT, Δ*mouR*, Δ*mouR*+*mouR* or Δ*mouR*+*mouR*(R44/48A) cultures in exponential growth in BHI medium at 37°C. Expression levels are represented relative to WT. Values are mean ± SD of three independent experiments. $^{**}P \leq 0.01$; $^{***}P \leq 0.001$. (**B**) Electrophoretic mobility shift assays of increasing amounts of purified MouR, MouR(R44/48A) or an unrelated putative regulator (Lmo0443) with a DNA fragment containing the promoter region of *agr* or *mouR*. Results are representative of at least three independent experiments. (**C**) Expression of *agrB* determined by RT-qPCR performed with total RNA isolated from *Lm* WT, Δ*mouR*+*mouR*(Y80F), Δ*mouR*+*mouR*(H133F) or Δ*mouR*+*mouR*(H134F) cultures in exponential growth in BHI medium at 37°C. Expression levels are represented relative to WT. Values are mean ± SD of three independent experiments.

alyzed the potential connection between MouR and these specific processes. We first confirmed that the *in vitro* growth of the WT, Δ*mouR* and Δ*mouR*+*mouR* strains was similar (Figure 6A). To test *Lm* chitinase activity, we spotted overnight cultures of the different strains on LB agar plates supplemented with chitin. The formation of a translucent halo on the opaque medium directly correlates with the bacterial chitinase activity (51). Our data showed that the mutant Δ*mouR* had a striking reduction in chitin hydrolysis when compared to both the WT and Δ*mouR*+*mouR* strains which, in turn, were comparable to each other (Figure 6B). A deletion mutant for *agrC* (Δ*agrC*), the sensor kinase component of the Agr system (72), showed undetectable chitin hydrolysis (Figure 6B). We also investigated the role of MouR in biofilm formation on PVC microplates by the crystal violet turbidimetry method (52). We observed that the Δ*mouR* mutant developed a significantly reduced biofilm relative to the WT strain, and that this defect was successfully reverted by gene complementation (Figure 6C). Again, the behaviour of Δ*agrC* further showed that the lack of a functional Agr system renders *Lm* unable to form a WT-like biofilm, thus confirming the relationship between MouR and biofilm formation. 3-D analysis of 3-day-old biofilms grown at 30°C on a glass surface confirmed that the *mouR* mutant formed a much thinner (maximal depth: WT = 14±2 μm; Δ*mouR* = 4±1 μm) and less dense biofilm than did the WT strain (Figure 6D).

Altogether, these results demonstrate how, by directly regulating the Agr system, MouR controls *Lm* chitinase activity and biofilm formation.

MouR is required for cell invasion and virulence

Taking into account the upregulation of *mouR* during *Lm* infection in mice and its role in chitinase activity and biofilm formation, we hypothesized that MouR could be important for the invasion of eukaryotic cells and establishment of systemic infection. To test this hypothesis, we infected the human cell lines Caco-2, Jeg-3 and HeLa with *Lm* WT and Δ*mouR* strains and assessed the number of intracellular bacteria. As compared to the WT strain, the Δ*mouR* mutant showed a slight defect in the invasion of all cell lines, especially in the case of Jeg-3 and HeLa cells (Figure 7A), suggesting a role for MouR in cell invasion. We then analyzed the potential role of MouR in intracellular multiplication by following the behavior of the WT and Δ*mouR* strains after internalization in RAW murine macrophage-like cells. Both strains grew with similar multiplication rates after uptake, indicating that *mouR* deletion has no consequence on intracellular multiplication (Figure 7B).

To investigate the role of MouR *in vivo,* mice were intravenously or orally infected with WT, Δ*mouR* or Δ*mouR*+*mouR* strains and the bacterial load per liver and spleen was assessed 72 h post-infection (Figure 7C and D). While no significant differences were detected in the bacterial burden of intravenously infected animals (Figure 7D), a significant reduction in the number of Δ*mouR* bacteria was observed in the liver of orally infected mice (Figure 7C). Furthermore, mice infected with the Δ*mouR*+*mouR* complemented strain showed bacterial levels comparable to the WT, revealing a restored phenotype (Figure 7C). *Lm* was previously shown to preferentially invade intestinal Peyer's patches following oral inoculation in the mouse model used in our study (73,74). We thus assessed numbers of *Lm* present in mouse Peyer's patches 72 h after oral inoculation. The results showed that invasion of intestinal Peyer's patches was less efficient in the absence of MouR (Figure 7E).

Altogether, our data indicate that MouR is necessary for *Lm* virulence in a mouse oral inoculation model, though not in an IV inoculation murine model.

DISCUSSION

Virulence regulators are crucial elements of the genome of pathogenic bacteria (10). They coordinate the transcriptional shift that mediates the switch from a saprophyte into a pathogen, granting the adaptability necessary to infect host organisms (6,7). It has been predicted that at least 209 transcription regulator-coding genes exist in the genome of *Lm* EGD-e (75). Whereas PrfA occupies the highest seat in the virulence regulation of *Lm*, controlling the expression of most of the main virulence factors (12), the identification of novel regulators is key to understand how *Lm* fine-tunes the expression of virulence determinants in order to optimally promote infection dissemination (12). In addition, despite the high abundance of transcription factors encoded in bacterial genomes, proper characterization of their 3D structures is limited (76,77). Here, we report the discovery and molecular characterization of a novel virulence regulator, MouR, along with the demonstration of its roles in the *Lm* virulence regulatory network as the transcriptional activator of the Agr system.

To our knowledge, this is the first regulator of the *Lm* Agr system identified. At least a dozen regulators have been linked to the activation and repression of *agr* in *S. aureus* (78). Although we do not rule out the existence of other regulators controlling Agr in *Lm* and also the existence of an autoregulation mechanism as suggested before (26,28), our data strongly indicate that MouR has an important role as activator of the Agr system.

By resolving the structure of MouR we opened ways to the classification and deeper characterization of this novel regulator. As initially predicted by bioinformatics, the crystal structure of MouR revealed that a monomer is composed of a typically conserved GntR N terminus with a winged-HTH DNA-binding domain and a variable C terminus with an E-O domain. Deeper analysis of the C-terminal structure led us to classify MouR as a member of the FadR sub-family, the largest sub-group of the GntR superfamily (19). The presence of exactly six α-helices within the C terminus allowed us to further classify it as a member of the VanR sub-class (79). Despite the large size of the FadR sub-family, currently making up close to 50% of all GntR proteins sequences on Pfam, only five VanR regulators are presently available in the PDB database (67,68,79). To our knowledge, this is the second GntR member (80) and the first VanR type regulator described in *Listeria*. Our structural data show that MouR is organized as a dimeric unit. GntR transcription factors predominantly bind their DNA–targets as dimers (79,81), however, the quaternary organization of these proteins and their mode of interac-

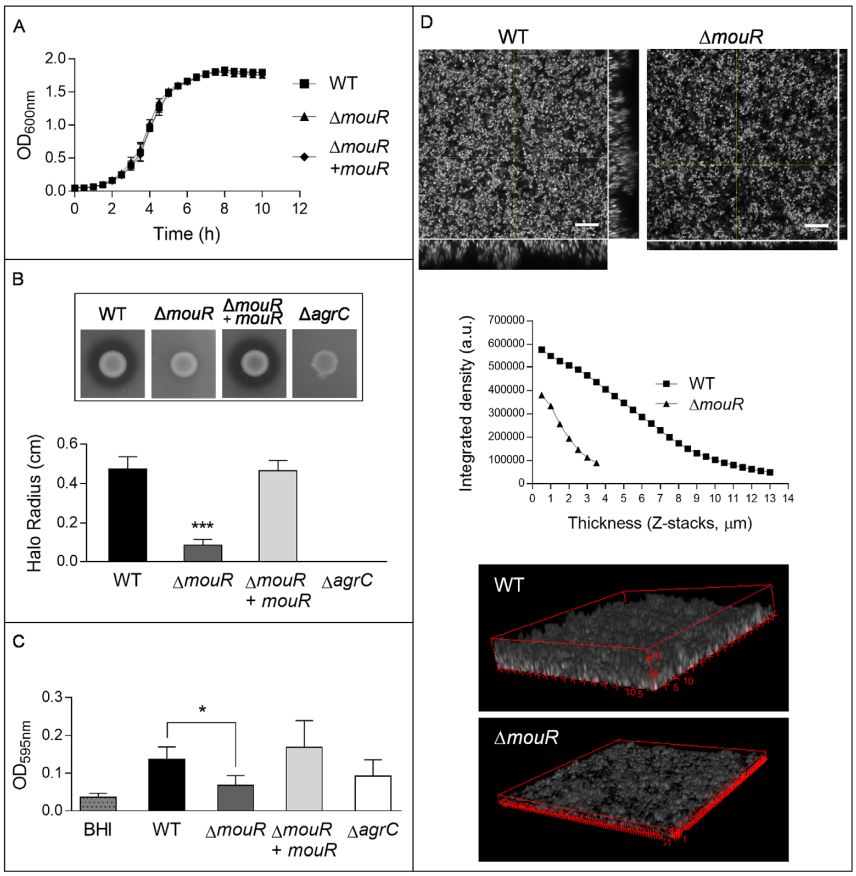

Figure 6. MouR regulates chitinase activity and biofilm formation. (**A**) Growth curves of different *Lm* strains in BHI. Overnight cultures were diluted 100-fold in BHI medium and incubated at 37°C with agitation. Measurement of optical density ($OD_{600\ nm}$) was performed every 30 min. (**B**) Chitinase activity of *Lm* WT, Δ*mouR*, Δ*mouR*+*mouR* and Δ*agrC*. Overnight cultures were spotted on LB agar plates supplemented with chitin and incubated at 30°C for 6 days. Halo measurements are mean ± SD of four independent experiments. (**C**) Biofilm formation of WT, Δ*mouR*, Δ*mouR*+*mouR* and Δ*agrC*. Cultures were diluted 100-fold in BHI, incubated in 96-well microplates for 20 h and biofilm formation was measured by the crystal violet assay. Wells with BHI medium served as control. Results are mean ± SD of three independent experiments. (**D**) Confocal microscopy images of *Lm* WT and Δ*mouR* biofilm developped on glass surface. Overnight cultures were diluted 100-fold in BHI medium and grown on glass coverslips at 30°C for three days. Bacteria were stained with acridine orange (0.1%) and imaged on a confocal microscope with a 0.5 µm z-stacking. Top: top view of fluorescent biofilm-forming bacteria, with x-z and y-z sagittal images on the right side and bottom of images, respectively. Lines indicate the planes corresponding to the sagittal images. Middle: Integrated density over biofilm thickness calculated from images above. Bottom: 3D model of a representative field from *Lm* WT and Δ*mouR* biofilms, created with Fiji-ImageJ. Florescence levels correlates to biofilm density and red lines indicate axis depth (µm). $*P \leq 0.05$; $***P \leq 0.001$.

tion with DNA vary across the family. Our structure and functional data show that the MouR dimer has a head-to-head orientation and that residues Arg44 and Arg48 in the α3-helices are involved in the interaction with DNA. The presence of a pocket in the C-terminal domain of MouR suggests the presence of an allosteric binding site. However, point mutations of the residues predicted to mediate the putative ligand binding did not impair MouR regulation of *agrB*, indicating that the presence of a ligand in this pocket is not crucial for *agr* transcriptional activation. Further studies should provide new insights about a possible modulation of MouR activity by ligand molecules.

Transcription factors can control gene expression in a direct or indirect fashion. This holds true in the case of *S. aureus* Agr as some of its regulators directly bind the *agr* promoter, while others have an indirect mode of control (78). Our results demonstrated the specific binding of MouR to the promoter region of the *agr* locus, thus indicating that *Lm* evolved a regulatory element to specifically control the Agr system. In addition, the incapacity of MouR to bind its own promoter suggests the absence of autoregulation, indicating that MouR could itself be controlled by unidentified regulators.

The Agr system was previously shown to have an impact on both *Lm* stress response/adaptation and pathogenicity, being in particular solidly linked to chitinase activity, biofilm formation and virulence (28). The Agr system promotes chitinase activity through negative regulation of the short ncRNA *lhrA,* which itself binds to chitinase mRNA (*chiA*) blocking ribosome access and translation (51,60). Furthermore, *Lm* chitinase has been established as a virulence factor involved in the modulation of the host immune system, through suppression of the hostile inducible nitric oxide synthase (iNOS) (82,83). Given the dual function of the chitinase and the regulatory role of MouR on the Agr system, it appears that MouR is involved in the adaptation of *Lm* to both the environment and the host. This could be

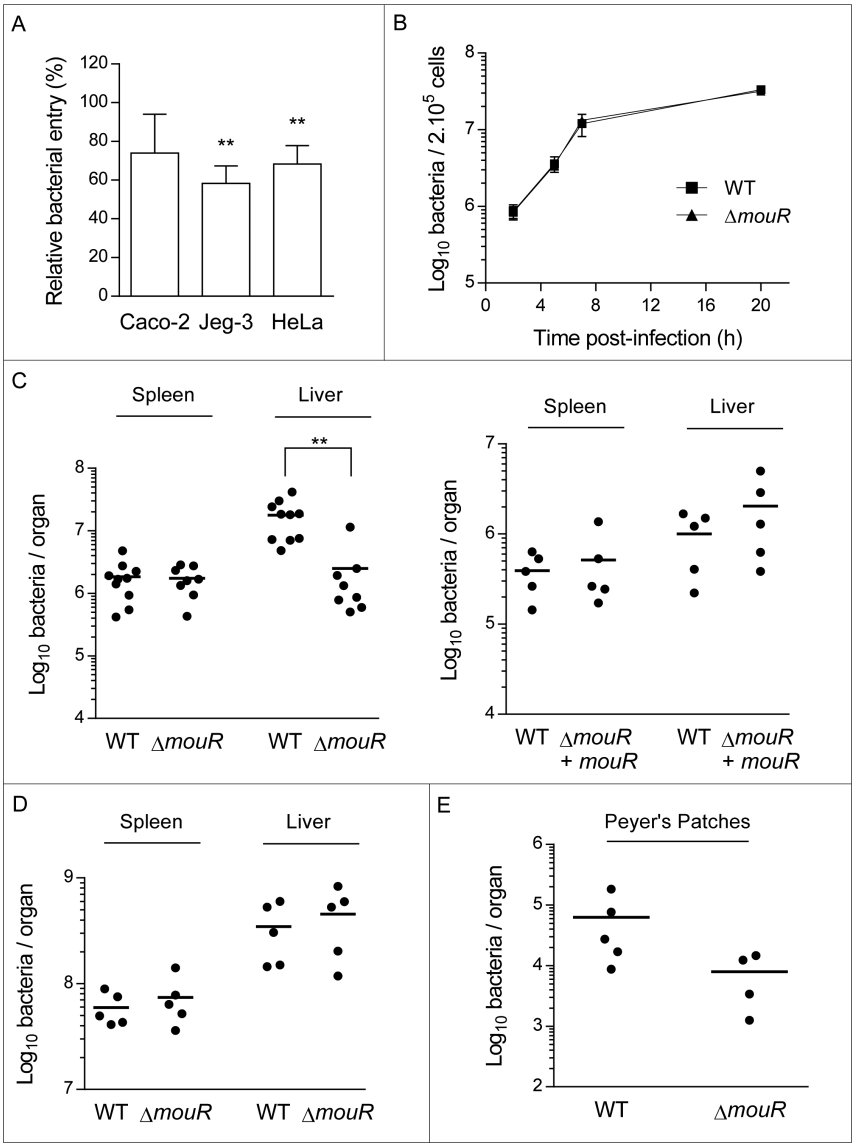

Figure 7. MouR is required for cell invasion and virulence. (**A**) Invasion of Caco-2, Jeg-3 and HeLa cell monolayers by *Lm* WT and Δ*mouR*, shown as intracellular CFU counts relative to WT (fixed at 100%). (**B**) Intracellular replication behaviour of the *Lm* WT and Δ*mouR* in RAW 264.7 cells. Results are mean ± SD of three independent experiments. CFU counts in spleens and livers of female BALB/c mice 72 h after (**C**) oral infection with 10^9 CFU of WT, Δ*mouR* or Δ*mouR*+*mouR* and (**D**) intravenous infection with 10^4 CFU of WT or Δ*mouR*. (**E**) CFU counts in Peyer's patches of female BALB/c mice 72 h after oral infection with 10^9 CFU of WT and Δ*mouR*. Each dot of the plot corresponds to one animal, mean values are represented by a horizontal bar. $^{**}P \leq 0.01$.

a factor contributing to the prevalence of a conserved *mouR* locus in pathogenic and non-pathogenic *Listeria* strains.

We also demonstrate here that MouR plays a role in the formation of *Lm* biofilm on abiotic surfaces. The relevance of biofilm formation in the context of *Lm* infection is not fully understood but it is a common general key feature for pathogen adaptation both outside and inside the host (84). Once established on surfaces or tools, biofilms drastically increase *Lm* survival, persistence and ultimately promote dissemination (85,86). The impact of the Agr system on biofilm formation in *Lm* has been shown before (26,87,88). Our data show that deletion of *mouR* does compromise biofilm formation to a similar extent of that of a Δ*agrC* mutant. The regulation of biofilm formation in bacteria is very complex. In *Lm,* the Agr system is only one of several regulatory elements that control biofilm formation, among which are the biofilm-promoting motility proteins flagellins (89) and the biofilm-repressing *luxS* signal transduction pathway (53). The orphan response regulator DegU has also been shown to play a role in *Lm* biofilm formation (90), partly independent of its control over flagella-related genes. In addition, a transcriptomics study revealed that DegU could positively control *mouR* expression at 24°C (18), adding another layer to the Agr-biofilm regulatory scene.

We show here that MouR appears to play a role in cell invasion. Previous studies have demonstrated that the expression of internalins InlA and InlB, as well as InlA allo-

cation to the membrane surface, are decreased in absence of a functional Agr system (28,88), inducing a defect of cell invasion (28,91). Although we did not detect a significant downregulation of *inlA/B* expression in absence of MouR, the invasion defect observed for the *mouR* deletion mutant could be related to a slight deregulation of *Lm* internalins due to impaired Agr functionality.

Importantly, we demonstrated that MouR is necessary for full *Lm* virulence in the mouse oral inoculation model. The absence of a defect in infectivity after intravenous inoculation points towards a role for MouR during the gastrointestinal phase of infection. In accordance, the *mouR* mutant infects less efficiently Peyer´s patches. The impaired ability to develop a biofilm in absence of MouR could possibly impact *Lm* prevalence in the digestive tract and the successful crossing of the intestinal barrier, as previously proposed (92). We also observed that the significantly decreased infectivity of the *mouR* mutant is only detected in mouse livers. A similar phenotype has been reported for a Δ*agrD* mutant where *Lm* was showed by bioluminescence to spread to the spleen but not the liver of infected mice (28). Considering the role of MouR and Agr on chitinase function, a differential modulation of iNOS/NO-based immune response in different organs could account for such differences. In a previous study, endotoxic shock in response to bacterial LPS induced different levels of iNOS expression in the spleen and the liver (93). Further studies could reveal a role for MouR/Agr in the modulation of the immune response in different organs and/or cell types.

We thus propose MouR as a dimeric DNA-binding transcription factor expressed by *Lm* that modulates, through the Agr system, biofilm formation and the host immune response, promoting bacterial virulence. This work reveals MouR as a new target for innovative strategies against *Lm* biofilm formation.

SUPPLEMENTARY DATA

Supplementary Data are available at NAR Online.

ACKNOWLEDGEMENTS

RT-qPCR technique was performed at the 'CCGen – Cell Culture and Genotyping' i3S Scientific Platform, with the assistance of Paula Magalhães and Tânia Meireles, and RNA-seq was performed at the 'GenCore – Genomics Core Facility' i3S Scientific Platform, with the assistance of Ana Mafalda Rocha. We are grateful for access to Proxima 2A at SOLEIL (Gif-sur-Yvette, France) and ID29 at ESRF (Grenoble, France) and thank the respective support staff. We are also very grateful to Prof. Rui Appelberg for PhD co-supervision of J.P., R.P. and F.C.

FUNDING

Norte-01-0145-FEDER-000012 – Structured program on bioengineered therapies for infectious diseases and tissue regeneration, supported by Norte Portugal Regional Operational Programme [NORTE 2020], under the PORTUGAL Partnership Agreement, through the European Regional Development Fund (FEDER); FCT Doctoral Fellowship [SFRH/BD/86871/2012, SFRH/BD/89542/2012, SFRH/BD/61825/2009 and SFRH/BD/112217/2015 to J.P., R.P., F.C. and C.B.] through FCT/MEC co-funded by QREN and POPH (Programa Operacional Potencial Humano); FCT Investigator program (COMPETE, POPH and FCT) (to S.S.). Funding for open access charge: Norte-01-0145-FEDER-000012 – Structured program on bioengineered therapies for infectious diseases and tissue regeneration, supported by Norte Portugal Regional Operational Programme [NORTE 2020].
Conflict of interest statement. None declared.

REFERENCES

1. Wu,H.J., Wang,A.H.J. and Jennings,M.P. (2008) Discovery of virulence factors of pathogenic bacteria. *Curr. Opin. Chem. Biol.*, **12**, 93–101.
2. McKenney,E.S. and Kendall,M.M. (2016) Microbiota and pathogen 'pas de deux': setting up and breaking down barriers to intestinal infection. *Pathog. Dis.*, **74**, 1–12.
3. Vasanthakrishnan,R.B., de las Heras,A., Scortti,M., Deshayes,C., Colegrave,N. and Vázquez-Boland,J.A. (2015) PrfA regulation offsets the cost of *Listeria* virulence outside the host. *Environ. Microbiol.*, **17**, 4566–4579.
4. Papenfort,K. and Vogel,J. (2010) Regulatory RNA in bacterial pathogens. *Cell Host Microbe*, **8**, 116–127.
5. Kepseu,W.D., Van Gijsegem,F. and Sepulchre,J.A. (2012) Modelling the onset of virulence in pathogenic bacteria. In: van Helden,J, Toussaint,A and Thieffry,D (eds). *Bacterial Molecular Networks: Methods and Protocols*. Springer, NY, 501–517.
6. Cossart,P. and Toledo-Arana,A. (2008) *Listeria monocytogenes*, a unique model in infection biology: an overview. *Microbes Infect.*, **10**, 1041–1050.
7. Camejo,A., Buchrieser,C., Couvé,E., Carvalho,F., Reis,O., Ferreira,P., Sousa,S., Cossart,P. and Cabanes,D. (2009) In vivo transcriptional profiling of *Listeria monocytogenes* and mutagenesis identify new virulence factors involved in infection. *PLoS Pathog.*, **5**, e1000449.
8. The European food safety authority and the European centre for disease prevention and control (2016) The European Union summary report on trends and sources of zoonoses, zoonotic agents and food-borne outbreaks in 2015. *EFSA J.*, **14**, 1–231.
9. Cossart,P. (2011) Illuminating the landscape of host-pathogen interactions with the bacterium *Listeria monocytogenes*. *Proc. Natl. Acad. Sci. U.S.A.*, **108**, 19484–19491.
10. Camejo,A., Carvalho,F., Reis,O., Leitão,E., Sousa,S. and Cabanes,D. (2011) The arsenal of virulence factors deployed by *Listeria monocytogenes* to promote its cell infection cycle. *Virulence*, **2**, 379–394.
11. Swaminathan,B. and Gerner-Smidt,P. (2007) The epidemiology of human listeriosis. *Microbes Infect.*, **9**, 1236–1243.
12. Freitag,N.E., Port,G.C. and Miner,M.D. (2009) *Listeria monocytogenes* — from saprophyte to intracellular pathogen. *Nat. Rev. Microbiol.*, **7**, 623–628.
13. Oliver,H.F., Orsi,R.H., Wiedmann,M. and Boor,K.J. (2010) *Listeria monocytogenes* σB has a small core regulon and a conserved role in virulence but makes differential contributions to stress tolerance across a diverse collection of strains. *Appl. Environ. Microbiol.*, **76**, 4216–4232.
14. Mandin,P., Fsihi,H., Dussurget,O., Vergassola,M., Milohanic,E., Toledo-Arana,A., Lasa,I., Johansson,J. and Cossart,P. (2005) VirR, a response regulator critical for *Listeria monocytogenes* virulence. *Mol. Microbiol.*, **57**, 1367–1380.
15. Christiansen,J.K., Larsen,M.H., Ingmer,H., Søgaard-Andersen,L. and Kallipolitis,B.H. (2004) The RNA-binding protein Hfq of *Listeria monocytogenes*: role in stress tolerance and virulence. *J. Bacteriol.*, **186**, 3355–3362.
16. Shen,A. and Higgins,D.E. (2006) The MogR transcriptional repressor regulates nonhierarchal expression of flagellar motility genes and virulence in *Listeria monocytogenes*. *PLoS Pathog.*, **2**, 282–295.
17. Kamp,H.D. and Higgins,D.E. (2009) Transcriptional and post-transcriptional regulation of the GmaR antirepressor governs

temperature-dependent control of flagellar motility in *Listeria monocytogenes*. *Mol. Microbiol.*, **74**, 421–435.
18. Williams,T., Joseph,B., Beier,D., Goebel,W. and Kuhn,M. (2005) Response regulator DegU of *Listeria monocytogenes* regulates the expression of flagella-specific genes. *FEMS Microbiol. Lett.*, **252**, 287–298.
19. Suvorova,I.A., Korostelev,Y.D. and Gelfand,M.S. (2015) GntR family of bacterial transcription factors and their DNA binding motifs: structure, positioning and co-evolution. *PLoS One*, **10**, e0132618.
20. Haydon,D.J. and Guest,J.R. (1991) A new family of bacterial regulatory proteins. *FEMS Microbiol. Lett.*, **63**, 291–295.
21. Hoskisson,P.A. and Rigali,S. (2009) Variation in form and function the helix-turn-helix regulators of the GntR superfamily. *Adv. Appl. Microbiol.*, **69**, 1–22.
22. van Aalten,D.M.F., DiRusso,C.C. and Knudsen,J. (2001) The structural basis of acyl coenzyme A-dependent regulation of the transcription factor FadR. *EMBO J.*, **20**, 2041–2050.
23. DiRusso,C.C., Black,P.N. and Weimar,J.D. (1999) Molecular inroads into the regulation and metabolism of fatty acids, lessons from bacteria. *Prog. Lipid Res.*, **38**, 129–197.
24. Novick,R.P. and Geisinger,E. (2008) Quorum sensing in Staphylococci. *Annu. Rev. Genet.*, **42**, 541–564.
25. Wuster,A. and Babu,M.M. (2008) Conservation and evolutionary dynamics of the *agr* cell-to-cell communication system across firmicutes. *J. Bacteriol.*, **190**, 743–746.
26. Rieu,A., Weidmann,S., Garmyn,D., Piveteau,P. and Guzzo,J. (2007) *agr* system of *Listeria monocytogenes* EGD-e: Role in adherence and differential expression pattern. *Appl. Environ. Microbiol.*, **73**, 6125–6133.
27. Autret,N., Raynaud,C., Dubail,I., Charbit,A. and Berche,P. (2003) Identification of the *agr* Locus of *Listeria monocytogenes*: role in bacterial virulence. *Infect. Immun.*, **71**, 4463–4471.
28. Riedel,C.U., Monk,I.R., Casey,P.G., Waidmann,M.S., Gahan,C.G.M. and Hill,C. (2009) AgrD-dependent quorum sensing affects biofilm formation, invasion, virulence and global gene expression profiles in *Listeria monocytogenes*. *Mol. Microbiol.*, **71**, 1177–1189.
29. Vivant,A.L., Garmyn,D., Gal,L. and Piveteau,P. (2014) The Agr communication system provides a benefit to the populations of *Listeria monocytogenes* in soil. *Front. Cell. Infect. Microbiol.*, **4**, 160.
30. Vivant,A.L., Garmyn,D., Gal,L., Hartmann,A. and Piveteau,P. (2015) Survival of *Listeria monocytogenes* in soil requires AgrA-mediated regulation. *Appl. Environ. Microbiol.*, **81**, 5073–5084.
31. Garmyn,D., Gal,L., Briandet,R., Guilbaud,M., Lemaître,J.P., Hartmann,A. and Piveteau,P. (2011) Evidence of autoinduction heterogeneity via expression of the Agr system of *Listeria monocytogenes* at the single-cell level. *Appl. Environ. Microbiol.*, **77**, 6286–6289.
32. Gray,B., Hall,P. and Gresham,H. (2013) Targeting *agr*- and *agr*-like quorum sensing systems for development of common therapeutics to treat multiple gram-positive bacterial infections. *Sensors*, **13**, 5130–5166.
33. Reis,O., Sousa,S., Camejo,A., Villiers,V., Gouin,E., Cossart,P. and Cabanes,D. (2010) LapB, a novel *Listeria monocytogenes* LPXTG surface adhesin, required for entry into eukaryotic cells and virulence. *J. Infect. Dis.*, **202**, 551–562.
34. Carvalho,F., Atilano,M.L., Pombinho,R., Covas,G., Gallo,R.L., Filipe,S.R., Sousa,S. and Cabanes,D. (2015) L-Rhamnosylation of *Listeria monocytogenes* wall teichoic acids promotes resistance to antimicrobial peptides by delaying interaction with the membrane. *PLoS Pathog.*, **11**, 1–29.
35. Pombinho,R., Camejo,A., Vieira,A., Reis,O., Carvalho,F., Almeida,M.T., Pinheiro,J.C., Sousa,S. and Cabanes,D. (2017) *Listeriamonocytogenes* CadC regulates cadmium efflux and fine-tunes lipoprotein localization to escape the host immune response and promote infection. *J. Infect. Dis.*, **215**, 1468–1479.
36. Arnaud,M., Chastanet,A. and Débarbouillé,M. (2004) New vector for efficient allelic replacement in naturally nontransformable, low-GC-content, Gram-positive bacteria. *Appl. Environ. Microbiol.*, **70**, 6887–6891.
37. Monk,I.R., Gahan,C.G.M. and Hill,C. (2008) Tools for functional postgenomic analysis of *Listeria monocytogenes*. *Appl. Environ. Microbiol.*, **74**, 3921–3934.
38. Benson,D.A., Cavanaugh,M., Clark,K., Karsch-Mizrachi,I., Lipman,D.J., Ostell,J. and Sayers,E.W. (2013) GenBank. *Nucleic Acids Res.*, **41**, 36–42.
39. Boratyn,G.M., Camacho,C., Cooper,P.S., Coulouris,G., Fong,A., Ma,N., Madden,T.L., Matten,W.T., McGinnis,S.D., Merezhuk,Y. *et al.* (2013) BLAST: a more efficient report with usability improvements. *Nucleic Acids Res.*, **41**, 29–33.
40. Sigrist,C.J.A., de Castro,E., Cerutti,L., Cuche,B.A., Hulo,N., Bridge,A., Bougueleret,L. and Xenarios,I. (2013) New and continuing developments at PROSITE. *Nucleic Acids Res.*, **41**, 344–347.
41. Marchler-Bauer,A., Bo,Y., Han,L., He,J., Lanczycki,C.J., Lu,S., Chitsaz,F., Derbyshire,M.K., Geer,R.C., Gonzales,N.R. *et al.* (2017) CDD/SPARCLE: Functional classification of proteins via subfamily domain architectures. *Nucleic Acids Res.*, **45**, D200–D203.
42. Kumar,S., Stecher,G. and Tamura,K. (2016) MEGA7: molecular evolutionary genetics analysis version 7.0 for bigger datasets. *Mol. Biol. Evol.*, **33**, 1870–1874.
43. Pinheiro,J., Reis,O., Vieira,A., Moura,I.M., Zanolli Moreno,L., Carvalho,F., Pucciarelli,M.G., García-del Portillo,F., Sousa,S. and Cabanes,D. (2017) *Listeria monocytogenes* encodes a functional ESX-1 secretion system whose expression is detrimental to in vivo infection. *Virulence*, **8**, 993–1004.
44. Kim,D., Pertea,G., Trapnell,C., Pimentel,H., Kelley,R. and Salzberg,S.L. (2013) TopHat2: accurate alignment of transcriptomes in the presence of insertions, deletions and gene fusions. *Genome Biol.*, **14**, R36.
45. Trapnell,C., Williams,B.A., Pertea,G., Mortazavi,A., Kwan,G., van Baren,M.J., Salzberg,S.L., Wold,B.J. and Pachter,L. (2011) Transcript assembly and abundance estimation from RNA-Seq reveals thousands of new transcripts and switching among isoforms. *Nat. Biotechnol.*, **28**, 511–515.
46. Trapnell,C., Roberts,A., Goff,L., Pertea,G., Kim,D., Kelley,D.R., Pimentel,H., Salzberg,S.L., Rinn,J.L. and Pachter,L. (2013) Differential gene and transcript expression analysis of RNA-seq experiments with TopHat and Cufflinks. *Nat. Protoc.*, **7**, 562–578.
47. Glomski,I.J., Gedde,M.M., Tsang,A.W., Swanson,J.A. and Portnoy,D.A. (2002) The *Listeria monocytogenes* hemolysin has an acidic pH optimum to compartmentalize activity and prevent damage to infected host cells. *J. Cell Biol.*, **156**, 1029–1038.
48. Kabsch,W. (1993) Automatic processing of rotation diffraction data from crystals of initially unknown symmetry land cell constants. *J. Appl. Crystallogr.*, **26**, 795–800.
49. Schneider,T.R. and Sheldrick,G.M. (2002) Substructure solution with SHELXD. *Acta Crystallogr. Sect. D Biol. Crystallogr.*, **58**, 1772–1779.
50. Adams,P.D., Afonine,P.V., Bunkóczi,G., Chen,V.B., Davis,I.W., Echols,N., Headd,J.J., Hung,L.W., Kapral,G.J., Grosse-Kunstleve,R.W. *et al.* (2010) PHENIX: A comprehensive Python-based system for macromolecular structure solution. *Acta Crystallogr. D. Biol. Crystallogr.*, **66**, 213–221
51. Paspaliari,D.K., Mollerup,M.S., Kallipolitis,B.H., Ingmer,H. and Larsen,M.H. (2014) Chitinase expression in *Listeria monocytogenes* is positively regulated by the Agr system. *PLoS One*, **9**, 1–8.
52. Christensen,G.D., Simpson,W.A., Younger,J.J., Baddour,L.M., Barrett,F.F., Melton,D.M. and Beachey,E.H. (1985) Adherence of coagulase-negative staphylococci to plastic tissue culture plates: A quantitative model for the adherence of staphylococci to medical devices. *J. Clin. Microbiol.*, **22**, 996–1006.
53. Sela,S., Frank,S., Belausov,E. and Pinto,R. (2006) A mutation in the *luxS* gene influences *Listeria monocytogenes* biofilm formation. *Appl. Environ. Microbiol.*, **72**, 5653–5658.
54. Schindelin,J., Arganda-Carreras,I., Frise,E., Kaynig,V., Longair,M., Pietzsch,T., Preibisch,S., Rueden,C., Saalfeld,S., Schmid,B. *et al.* (2012) Fiji: an open-source platform for biological-image analysis. *Nat. Methods*, **9**, 676–682.
55. Rueden,C.T., Schindelin,J., Hiner,M.C., DeZoina,B.E., Walter,A.E., Arena,E.T. and Eliceiri,W. (2017) ImageJ2: ImageJ for the next generation of scientific image data. *BMC Bioinform.*, **18**, 529.
56. Cabanes,D., Lecuit,M. and Cossart,P. (2008) Animal models of *Listeria* infection. *Curr. Protoc. Microbiol.*, doi:10.1002/9780471729259.mc09b01s10.
57. Toledo-Arana,A., Dussurget,O., Nikitas,G., Sesto,N., Guet-Revillet,H., Balestrino,D., Loh,E., Gripenland,J., Tiensuu,T.,

Vaitkevicius,K. *et al.* (2009) The *Listeria* transcriptional landscape from saprophytism to virulence. *Nature*, **459**, 950–956.
58. Garmyn,D., Gal,L., Lemaitre,J.P., Hartmann,A. and Piveteau,P. (2009) Communication and autoinduction in the species *Listeria monocytogenes*: A central role for the *agr* system. *Commun. Integr. Biol.*, **2**, 371–374.
59. Nielsen,J.S., Lei,L.K., Ebersbach,T., Olsen,A.S., Klitgaard,J.K., Valentin-Hansen,P. and Kallipolitis,B.H. (2009) Defining a role for Hfq in Gram-positive bacteria: Evidence for Hfq-dependent antisense regulation in *Listeria monocytogenes*. *Nucleic Acids Res.*, **38**, 907–919.
60. Nielsen,J.S., Larsen,M.H., Lillebæk,E.M.S., Bergholz,T.M., Christiansen,M.H.G., Boor,K.J., Wiedmann,M. and Kallipolitis,B.H. (2011) A small RNA controls expression of the chitinase ChiA in *Listeria monocytogenes*. *PLoS One*, **6**, e19019.
61. Gopal,S., Berg,D., Hagen,N., Schriefer,E.M., Stoll,R., Goebel,W. and Kreft,J. (2010) Maltose and maltodextrin utilization by *Listeria monocytogenes* depend on an inducible ABC transporter which is repressed by glucose. *PLoS One*, **5**, e10349.
62. Deutscher,J., Aké,F.M.D., Zébré,A.C., Cao,T.N., Kentache,T., Monniot,C., Pham,Q.M.M., Mokhtari,A., Joyet,P., Milohanic,E. *et al.* (2014) Carbohydrate utilization by *Listeria monocytogenes* and its influence on virulence gene expression. In: Hambrick,EC (ed). *Listeria Monocytogenes: Food Sources, Prevalence and Management Strategies*. Nova Science Publishers, pp. 49–76.
63. Chatterjee,S.S., Hossain,H., Otten,S., Kuenne,C., Kuchmina,K., Machata,S., Domann,E., Chakraborty,T. and Hain,T. (2006) Intracellular gene expression profile of *Listeria monocytogenes*. *Infect. Immun.*, **74**, 1323–1338.
64. Joseph,B., Przybilla,K., Stühler,C., Slaghuis,J., Fuchs,T.M., Goebel,W., Stu,C. and Schauer,K. (2006) Identification of *Listeria monocytogenes* genes contributing to intracellular replication by expression profiling and mutant screening. *J. Bacteriol.*, **188**, 556–568.
65. Zhang,Y. and Skolnick,J. (2005) TM-align: a protein structure alignment algorithm based on the TM-score. *Nucleic Acids Res.*, **33**, 2302–2309.
66. Krissinel,E. and Henrick,K. (2007) Inference of macromolecular assemblies from crystalline state. *J. Mol. Biol.*, **372**, 774–797.
67. Zheng,M., Cooper,D.R., Grossoehme,N.E., Yu,M., Hung,L.W., Cieslik,M., Derewenda,U., Lesley,S.A., Wilson,I.A., Giedroc,D.P. *et al.* (2009) Structure of *Thermotoga maritima* TM0439: Implications for the mechanism of bacterial GntR transcription regulators with Zn2+-binding FCD domains. *Acta Crystallogr. Sect. D Biol. Crystallogr.*, **65**, 356–365.
68. Lord,D.M., Baran,A.U., Soo,V.W.C., Wood,T.K., Peti,W. and Page,R. (2014) McbR/YncC: implications for the mechanism of ligand and DNA binding by a bacterial GntR transcriptional regulator involved in biofilm formation. *Biochemistry*. **53**, 7223–7231.
69. Xu,Y., Heath,R.J., Li,Z., Rock,C.O. and White,S.W. (2001) The FadR·DNA complex. *J. Biol. Chem.*, **276**, 17373–17379.
70. Shi,W., Kovacikova,G., Lin,W., Taylor,R.K., Skorupski,K. and Kull,F.J. (2015) The 40-residue insertion in *Vibrio cholerae* FadR facilitates binding of an additional fatty acyl-CoA ligand. *Nat. Commun.*, **6**, 6032.
71. Gajiwala,K.S. and Burley,S.K. (2000) Winged helix proteins. *Curr. Opin. Struct. Biol.*, **10**, 110–116.
72. Pöntinen,A., Markkula,A., Lindström,M. and Korkeala,H. (2015) Two-component-system histidine kinases involved in growth of *Listeria monocytogenes* EGD-e at low temperatures. *Appl. Environ. Microbiol.*, **81**, 3994–4004.
73. Chiba,S., Nagai,T., Hayashi,T., Baba,Y., Nagai,S. and Koyasu,S. (2011) Listerial invasion protein internalin B promotes entry into ileal Peyer's patches *in vivo*. *Microbiol. Immunol.*, **55**, 123–129.
74. Gessain,G., Tsai,Y., Travier,L., Bonazzi,M., Grayo,S., Cossart,P., Charlier,C., Disson,O. and Lecuit,M. (2015) PI3-kinase activation is critical for host barrier permissiveness to *Listeria monocytogenes*. *J. Exp. Med.*, **212**, 165–183.
75. Glaser,P., Frangeul,L., Buchrieser,C., Rusniok,C., Amend,A., Baquero,F., Berche,P., Bloecker,H., Brandt,P., Chakraborty,T. *et al.* (2001) Comparative genomics of *Listeria* species. *Science*, **294**, 849–852.
76. Seshasayee,A.S.N., Sivaraman,K. and Luscombe,N.M. (2011) An overview of prokaryotic transcription factors. In: Hughes,TR (ed). *A Handbook of Transcription Factors*. Springer, Netherlands, pp. 7–23.
77. Rodionov,D.A. (2007) Comparative genomic reconstruction of transcription regulatory networks in bacteria. *Chem. Rev.*, **107**, 3467–3497.
78. Thoendel,M., Kavanaugh,J.S., Flack,C.E. and Horswill,A.R. (2011) Peptide signaling in the staphylococci. *Chem. Rev.*, **111**, 117–151.
79. Jain,D. (2015) Allosteric control of transcription in GntR family of transcription regulators: a structural overview. *IUBMB Life*, **67**, 556–563.
80. Wassinger,A., Zhang,L., Tracy,E., Munson,R.S., Kathariou,S. and Wang,H.H. (2013) Role of a GntR-family response regulator LbrA in *Listeria monocytogenes* biofilm formation. *PLoS One*, **8**, 1–7.
81. Rigali,S., Derouaux,A., Giannotta,F. and Dusart,J. (2002) Subdivision of the helix-turn-helix GntR family of bacterial regulators in the FadR, HutC, MocR, and YtrA subfamilies. *J. Biol. Chem.*, **277**, 12507–12515.
82. Chaudhuri,S., Gantner,B.N., Ye,R.D., Cianciotto,N.P. and Freitag,N.E. (2013) The *Listeria monocytogenes* ChiA chitinase enhances virulence through suppression of host innate immunity. *MBio*, **4**, 1–9.
83. Frederiksen,R.F., Paspaliari,D.K., Larsen,T., Storgaard,B.G., Larsen,M.H., Ingmer,H., Palcic,M.M. and Leisner,J.J. (2013) Bacterial chitinases and chitin-binding proteins as virulence factors. *Microbiol.*, **159**, 833–847.
84. Jamal,M., Ahmad,W., Andleeb,S., Jalil,F., Imran,M., Nawaz,M.A., Hussain,T., Ali,M., Rafiq,M. and Kamil,M.A. (2017) Bacterial biofilm and associated infections. *J. Chinese Med. Assoc.*, **81**, 7–11.
85. Møretrø,T. and Langsrud,S. (2004) *Listeria monocytogenes*: biofilm formation and persistence in food-processing environments. *Biofilms*, **1**, 107–121.
86. Colagiorgi,A., Bruini,I., Di Ciccio,P.A., Zanardi,E., Ghidini,S. and Ianieri,A. (2017) *Listeria monocytogenes* biofilms in the wonderland of food industry. *Pathogens*, **6**, 41.
87. Rieu,A., Briandet,R., Habimana,O., Garmyn,D., Guzzo,J. and Piveteau,P. (2008) *Listeria monocytogenes* EGD-e biofilms: No mushrooms but a network of knitted chains. *Appl. Environ. Microbiol.*, **74**, 4491–4497.
88. Garmyn,D., Augagneur,Y., Gal,L., Vivant,A.L. and Piveteau,P. (2012) *Listeria monocytogenes* differential transcriptome analysis reveals temperature-dependent Agr regulation and suggests overlaps with other regulons. *PLoS One*, **7**, e43154.
89. Vatanyoopaisarn,S., Nazli,A., Dodd,C.E.R., Rees,C.E.D. and Waites,W.M. (2000) Effect of flagella on initial attachment of *Listeria monocytogenes* to stainless steel. *Am. Soc. Microbiol.*, **66**, 860–863.
90. Gueriri,I., Cyncynatus,C., Dubrac,S., Arana,A.T., Dussurget,O. and Msadek,T. (2008) The DegU orphan response regulator of *Listeria monocytogenes* autorepresses its own synthesis and is required for bacterial motility, virulence and biofilm formation. *Microbiol.*, **154**, 2251–2264.
91. Zetzmann,M., Sánchez-Kopper,A., Waidmann,M.S., Blombach,B. and Riedel,C.U. (2016) Identification of the *agr* peptide of *Listeria monocytogenes*. *Front. Microbiol.*, **7**, 1–11.
92. Begley,M., Kerr,C. and Hill,C. (2009) Exposure to bile influences biofilm formation by *Listeria monocytogenes*. *Gut Pathog.*, **1**, 11.
93. Kan,W., Zhao,K., Jiang,Y., Yan,W., Huang,Q., Wang,J., Qin,Q., Huang,X. and Wang,S. (2004) Lung, spleen, and kidney are the major places for inducible nitric oxide synthase expression in endotoxic shock: role of p38 mitogen-activated protein kinase in signal transduction of inducible nitric oxide synthase expression. *Shock*, **21**, 281–287.